ISSN: 2230-9926

Available online at http://www.journalijdr.com

IJDR

International Journal of Development Research
Vol. 08, Issue, 05, pp.20535-20543, May, 2018

ORIGINAL RESEARCH ARTICLE OPEN ACCESS

A NEW APPROACH TO SOLVE THE TIME-DEPENDENT THREE-DIMENSIONAL ADVECTION-DIFFUSION EQUATION APPLIED TO MODEL AIR POLLUTION DISPERSION IN THE PLANETARY BOUNDARY LAYER

***Glênio A. Gonçalves, Daniela Buske, Régis S. Quadros and Guilherme J. Weymar**

Graduate Program in Mathematical Modelling, Federal University of Pelotas, Pelotas, RS, Brazil.

ARTICLE INFO

Article History:

Received 25th February, 2018
Received in revised form
04th March, 2018
Accepted 17th April, 2018
Published online 31st May, 2018

Key Words:

Atmospheric Dispersion;
Analytical Solution;
Time-dependent Advection-Diffusion Equation; Air Pollution Modeling.

ABSTRACT

In this work we present an analytical solution for the time-dependent three-dimensional advection-diffusion equation to simulate the pollutant dispersion in the Planetary Boundary Layer (PBL). In this new approach the advection-diffusion equation is solved using a combination of the separation of variables and GILTT methods. The great advantage is that, by this way, we avoid the numerical inversion done in the previous works in literature using the GILTT method. We also report numerical simulations and statistical comparison with experimental data available in the literature.

Citation: Glênio A. Gonçalves, Daniela Buske, Régis S. Quadros and Guilherme J. Weymar, 2018. "A new approach to solve the time-dependent three-dimensional advection-diffusion equation applied to model air pollution dispersion in the planetary boundary layer", *International Journal of Development Research*, 8, (05), 20535-20543.

INTRODUCTION

During decades, great attention has been devoted to solve analytically the advection-diffusion equation with the purpose to simulate pollutant dispersion in atmosphere in a more realistic manner. A variety of solutions appeared in literature during these researches, but, in majority, the solutions are for very specific cases, considering constant or simple eddy diffusivities coefficients for example (Moreira *et al*., 2009). More recently, appeared the GILTT method which solves the time-dependent multidimensional advection-diffusion equation (Wortmann *et al*., 2005; Moreira *et al*., 2006; Moreira *et al*., 2009; Buske *et al*., 2012a, 2012b, 2016; Vilhena *et al*., 2012), assuming variable wind and eddy diffusivity coefficient.

The main idea of this methodology relies on the solution of the classical GITT transformed equations (Cotta and Mikhaylov, 1997) analytically, by the Laplace Transform technique. The time-dependent advection-diffusion equation is solved applying the Laplace Transform technique in the time variable (Moreira *et al*., 2006) and the stationary resulting equation is solved by the GILTT method. The final concentration is obtained by numerical inversion in time using Gaussian quadrature. In this work we step further, now solving the three-dimensional nonstationary advection-diffusion equation avoiding the numerical inversion done in the previous works in literature using the GILTT method. Such solution is obtained through a combination of the separation of variables and GILTT methods. The great advantage is that, by this way, we obtain the final pollutant concentration much faster. This paper is organized as follows: in section 2, we present the solution proposed for the advection-diffusion equation; in section

3, we briefly report the data set and parameterization considered in the simulations; in section 4, numerical simulations and statistical comparison with experimental data and with models available at literature are shown and discussed. Finally, in section 5, an analysis of the methodology proposed is done.

Solution of the advection-diffusion equation

The three-dimensional advection-diffusion equation, considering Fickian closure of turbulence, which describes, without loss of generality, the pollutant dispersion in the atmosphere, written as

$$\frac{\partial C}{\partial t}+u\frac{\partial C}{\partial x}=\frac{\partial}{\partial y}\left(K_y\frac{\partial C}{\partial y}\right)+\frac{\partial}{\partial z}\left(K_z\frac{\partial C}{\partial z}\right) \qquad \text{……..(1)}$$

where $C(t,x,y,z)$ denotes the function concentration (kg/m^3), K_y is the lateral eddy diffusivity (m^2/s), $K_z = K_z(z)$ is the vertical eddy diffusivity coefficient (m^2/s), u is the longitudinal mean wind component oriented in the x direction (m/s).

Equation (1) is subjected to the following boundary conditions

$$K_z\frac{\partial C}{\partial z}=0 \qquad \text{at } z=0,\ h \qquad \text{……(2.a)}$$

initial condition,

$$u\,C(0,x,y,z)=Q(0)\delta(x)\delta(y)\delta(z-H_s) \qquad \text{……..(2.b)}$$

and the source condition

$$u\,C(t,0,y,z)=Q(t)\delta(y)\delta(z-H_s) \qquad \text{……(2.c)}$$

where h (m) is the boundary layer height, H_s (m) the source height and Q (g/m^2) is the source intensity.

Proceeding with the variable separation of the differential equation (1), considering initially that u e K_y are constant,

$$\frac{d}{dt}T_{\kappa\lambda}=-(\kappa^2K_y+\lambda)T_{\kappa\lambda} \qquad \text{……..(3.a)}$$

$$u\frac{d}{dx}X_{\alpha\lambda}=(\alpha+\lambda)X_{\alpha\lambda} \qquad \text{……...(3.b)}$$

$$\frac{d^2}{dy^2}\mathrm{Y}_\kappa=-\kappa^2\,\mathrm{Y}_\kappa \qquad \text{……(3.c)}$$

$$\frac{d}{dz}\left(K(z)\frac{d}{dz}Z_\alpha\right)=\alpha\ \frac{d}{dx}Z_\alpha \qquad \text{……..(3.d)}$$

where eigenvalues are presented in a more convenient form. By this way the solution for equation (3.a) is given by

$$T_{\kappa\lambda}(t)=T_\kappa(t)\,T_\lambda(t)=e^{-\kappa^2K_yt}\ e^{-\lambda t}, \qquad \text{……(4)}$$

the solution for equation (3.b) is

$$\mathrm{X}_{\alpha\lambda}(x)=\mathrm{X}_\alpha(x)\mathrm{X}_\lambda(x)=e^{\frac{(\alpha+\lambda)}{u}x}=e^{\frac{\alpha x}{u}}e^{\frac{\lambda x}{u}},$$
$$\text{……(5)}$$

and solution for equation (3.c) is

$$\mathrm{Y}_\kappa(y)=A(\kappa)\cos(\kappa\ y) \qquad \text{……(6)}$$

The solution for equation (3.d) is obtained by the well-known GILTT method (Moreira *et al*., 2009; Buske *et al*., 2012a).

Finally, the problem solution is given in a product form like

$$C_{k\lambda\alpha}(t,x,y,z) = \left[T_\kappa(t)\mathrm{Y}_\kappa(y)\right]\left[T_\lambda(t)\mathrm{X}_\lambda(x)\right]\left[\mathrm{X}_\alpha(x)GILTT_\alpha(z)\right] \quad \text{.....(7)}$$

Looking each factor of equation (7) separately, using equations (4)-(6), is possible to write

$$\psi_\kappa(t,y) = T_\kappa(t)\mathrm{Y}_\kappa(y) = A(\kappa)e^{-\kappa^2 K_y t}\cos(\kappa y) \quad \text{.....(8)}$$

$$\varphi_\lambda(t,x) = T_\lambda(t)\mathrm{X}_\lambda(x) = e^{-\lambda t}e^{\frac{\lambda x}{u}}e^{\lambda t} = e^{-\frac{\lambda}{u}(ut-x)} \quad \text{.....(9)}$$

$$\frac{\partial}{\partial z}\left(K(z)\frac{\partial}{\partial z}\phi_\alpha(x,z)\right) = u\frac{\partial}{\partial x}\phi_\alpha(x,z) \quad \text{.....(10)}$$

where $\phi_\alpha(x,z) = \mathrm{X}_\alpha(x)GILTT_\alpha(z)$. By this way, equation (7) is rewritten as

$$C_{k\lambda\alpha}(t,x,y,z) = \psi_\kappa(t,y)\varphi_\lambda(t,x)\phi_\alpha(x,z) \quad \text{.....(11)}$$

Once the domain is infinite in x and y the eigenvalues are continuous, the solution for the concentration C is given by:

$$C(t,x,y,z) = \int_0^\infty A(\kappa)\psi_\kappa(t,y)d\kappa \int_0^\infty B(\lambda)\varphi_\lambda(t,x)d\lambda \;\; GILTT(x,z) \quad \text{.....(12)}$$

and once the eigenvalues κ(m) and λ(1/s) are considered continuous in $[0,\infty)$, the final concentration is expressed as

$$C(t,x,y,z) = \psi(t,y)\,\varphi(t,x)\,GILTT(x,z) \quad \text{.....(13)}$$

where

$$\psi(t,y) = \int_0^\infty A(\kappa)\psi_\kappa(t,y)d\kappa \;,\; \varphi(t,x) = \int_0^\infty B(\lambda)\varphi_\lambda(t,x)d\lambda \quad \text{and} \quad GILTT(x,z) = \int_0^\infty C(\alpha)GILTT_\alpha(x,z)d\alpha$$

To determine the functions $\psi(t,y)$ and $\varphi(t,x)$ the initial and source conditions are used. The function $GILTT(x,z)$ comes from the solution obtained by the GILTT method (Moreira *et al*., 2009; Buske *et al*., 2012a). The development to determine $\psi(t,y)$ and $\varphi(t,x)$ is shown in the sequence.

To solve $\psi(t,y) = \int_0^\infty A(\kappa)\psi_\kappa(t,y)$, the initial condition (2.b) is used. Taking

$$u\,C(0,x,y,z) = Q(0)\delta(x)\delta(y)\delta(z-H_s) = u\,\psi(0,y)\,\varphi(0,x)\,GILTT(x,z) \quad \text{.....(14)}$$

is possible to stablish that $\begin{cases} \psi(0,y) = \delta(y) \\ \varphi(0,x) = Q(0)\delta(x) \\ GILTT(x,z) = \delta(z-H_s)/u \end{cases}$, and then find the integral related to the eigenvalue κ.

Taking only the term related to the integral that composes the solution, using equation (8),

$$\psi(t,y) = \int_0^\infty A(\kappa)\psi_\kappa(t,y) = \int_0^\infty A(\kappa)e^{-K_y\kappa^2 t}\cos(\kappa y)d\kappa \quad \text{.....(15)}$$

Is possible to note, from equation (15), that $\psi(t,y)$ can be written as a Fourier Cosines transform, more exactly like:

$$\psi(t,y) = \sqrt{\frac{2}{\pi}}\int_0^\infty \Phi(\kappa,t)\cos(\kappa y)d\kappa \quad \text{.....(16)}$$

with $\Phi(\kappa,t) = \sqrt{\frac{\pi}{2}}A(\kappa)e^{-K_y\kappa^2 t}$. Appling the formula for the inversion of Fourier Cosines Transform in the previous equation (16), and the initial condition, is found $A(\kappa) = \frac{2}{\pi}$. Thus equation (16) is written as

$$\psi(t,y)=\frac{2}{\pi}\int_0^{\infty} e^{-K_y\kappa^2 t}\cos(\kappa y)d\kappa=\frac{2}{\sqrt{4\pi K_y t}}e^{-\frac{y^2}{4K_y t}} \quad \text{.....(17)}$$

To solve $\varphi(t,x)=\int_0^{\infty}B(\lambda)\varphi_\lambda(t,x)d\lambda$, the source condition (2.c) is used. Taking

$$u\,C(t,0,y,z)=Q(t)\delta(y)\delta(z-H_s)=u\psi(t,y)\,\varphi(t,0)\,GILTT(0,z) \ , \quad \text{.....(18)}$$

integrating this condition in the variable y,

$$Q(t)\delta(z-H_s)=\varphi(t,0)\,u\,GILTT(0,z) \quad \text{.....(19)}$$

and establishing the equalities $\begin{cases}\varphi(t,0)=Q(t)\\ GILTT(0,z)=\delta(z-H_s)/u\end{cases}$, is possible to find the integral related to the eigenvalue λ.

Again, taking only the term related to the integral that composes the solution, using equation (09),

$$\varphi(t,x)=\int_0^{\infty}B(\lambda)\varphi_\lambda(t,x)d\lambda=\int_0^{\infty}B(\lambda)e^{-\frac{\lambda}{u}(ut-x)}d\lambda=\int_0^{\infty}B(\lambda)e^{\lambda\frac{x}{u}}e^{-\lambda t}d\lambda \quad \text{.....(20)}$$

By considering the source condition at x = 0, $\varphi(t,0)=\int_0^{\infty}B(\lambda)e^{-\lambda t}d\lambda$, and then applying the inverse of Laplace transform, the constants $B(\lambda)$ are determined and given by

$$\varphi(t,x)=\int_0^{\infty}L^{-1}\{Q(t),t\to\lambda\}e^{-\lambda\left(t-\frac{x}{u}\right)}d\lambda=Q\left(t-\frac{x}{u}\right) \quad \text{..... (21)}$$

Finally, the solution will be the product of equations (17), (21) and the GILTT solution, that is

$$C(t,x,y,z)=\frac{2}{\sqrt{4\pi K_y t}}e^{-\frac{y^2}{4K_y t}}\,Q\left(t-\frac{x}{u}\right)\,GILTT(x,z) \quad \text{.....(22)}$$

The idea to obtain the solution of GILTT(x,z), briefly speaking, comprehends the steps: expansion of the concentration in series of eigenfunctions attained from an auxiliary problem, replacing this equation in the advection-diffusion equation and taking moments, one comes out with a matrix ordinary differential equation that is then solved analytically by the Laplace Transform technique. For more information see the works of Wortmann *et al*. (2005), Moreira *et al*. (2006, 2009), Buske *et al*. (2012a, 2012b, 2016).

Analytical Solution – Plume Solution

It is important to emphasize that the solution using a Dirac delta function source is a Green's solution. This means that by knowing Green's solution, we can find solutions with different forms of time-dependent sources through the superposition principle for linear operator problems. For this, the Dirac delta source will be of the form $\delta(t-\tau)$. If a function strongly concentrated with the property $\delta(t)=\lim_{b\to 0}\frac{1}{\sqrt{\pi b}}e^{-\frac{t^2}{b}}$ is considered, is easy to see that $\delta\left((t-\tau)-\frac{x}{u}\right)=\lim_{b\to 0}\frac{u}{\sqrt{\pi b u^2}}e^{-\frac{((t-\tau)-x/u)^2}{b}}$, or, in a more convenient form $\delta\left((t-\tau)-\frac{x}{u}\right)=\lim_{b\to 0}\frac{u}{\sqrt{\pi b u^2}}e^{-\frac{(u(t-\tau)-x)^2}{bu^2}}$. Assuming that $b=(4K_x t)/u^2$, is possible to write

$$Q\,\delta\left((t-\tau)-\frac{x}{u}\right)=\lim_{K_x\to 0}\frac{Mu}{\sqrt{4\pi K_x t}}e^{-\frac{(u(t-\tau)-x)^2}{4K_x t}} \quad \text{.....(23)}$$

In order to allow the solution to consider the diffusion process in the longitudinal direction, the limit is relaxed for K_x . Thus, through equation (23), the Green solution is written as:

$$G(t,\tau,x,y,z)=\frac{2Mu}{\sqrt{16\pi^2 K_x K_y t^2}}\, e^{-\frac{y^2}{4K_y t}}\, e^{-\frac{(u(t-\tau)-x)^2}{4K_x t}}\; GILTT(x,z)$$

……(24)

At this point, if is considered a problem with arbitrary source $Q(t)$ emitting at an interval (t_0, t) , the solution to the problem through the superposition principle is given by τ integration over interval $[t_0, t]$. In a particular case, the plume solution can be constructed using the Heaviside function as the source:

$$C(t,x,y,z)=\frac{2uQ\, e^{-\frac{y^2}{4K_y t}}}{\sqrt{16\pi^2 K_x K_y t^2}}\int_0^t e^{-\frac{(u(t-\tau)-x)^2}{4K_x t}}\, d\tau\; GILTT(x,z)$$

……(25)

where $M = Qd\tau$ is the mass released in time interval *t* and t_0 is equal to zero.

$$C(t,x,y,z)=\frac{Q\, e^{-\frac{y^2}{4K_y t}}}{\sqrt{4\pi K_y t}}\left[erf\left(\frac{ut-x}{4K_x t}\right)-erf\left(\frac{-x}{4K_x t}\right)\right] GILTT(x,z)$$

……...(26)

in which *erf* is the error function.

Boundary Layer Parameterization

With the purpose of comparison with results of the literature, the boundary layer parameterization was chosen as the same adopted by the authors Moreira *et al*. (2006, 2009), Buske *et al*. (2012a, 2012b, 2016). In terms of the convective scaling parameters the vertical eddy diffusivity can be formulated as (Degrazia *et al*., 1997):

$$\frac{K_z}{w_* h}=0.22\left(\frac{z}{h}\right)^{1/3}\left(1-\frac{z}{h}\right)^{1/3}\left[1-\exp\left(-\frac{4z}{h}\right)-0.0003\exp\left(\frac{8z}{h}\right)\right]$$

……..(27)

For the lateral eddy diffusivities, a formulation given by Seinfeld and Pandis (1998) was used:

$$K_\alpha = 0.1 w_* h$$

……..(28)

where α represents *x* and *y* directions respectively.

The wind speed profile can be described by a power law expressed as follows (Panofsky and Dutton, 1988):

$$u_z = u_1\left(\frac{z}{z_1}\right)^n$$

.....(29)

where u_z and u_1 are the mean wind speeds horizontal to heights *z* and z_1 and *n* is an exponent that is related to the intensity of turbulence (Irwin, 1979). Here, for the unstable case studied, *n*=0.1 was adopted.

Numerical Simulations

The performance of the new approach was evaluated with the boundary layer parameterization proposed, using the crosswind integrated equation (26) and the data set of the diffusion Copenhagen experiment (Gryning and Lyck, 1984). The Copenhagen data set is composed of tracer SF_6 data from dispersion experiments carried out in northern Copenhagen. The tracer was released without buoyancy from a tower at a height of 115 m and was collected at ground-level positions in up to three crosswind arcs of tracer sampling units. The sampling units were positioned 2-6 km far from the point of release. Tracer releases typically started up 1 hour before the tracer sampling and stopped at the end of the sampling period. The site was mainly residential with a roughness length of 0.6 m. In this work two situations were considered in the analysis of the results obtained using the Copenhagen data set. First, were used the values of the ground-level crosswind integrated concentrations normalized with the tracer release rate from

Gryning *et al*. (1987). In this case the distributed data set contains hourly mean values of concentrations and meteorological data. Second, data with a greater time resolution were considered as suggested by Tirabassi and Rizza (1997): 20 minutes averaged measured concentrations and 10 minutes averaged values for meteorological data. Tables 1, 2 and 3 report the friction velocity u_* , the Monin-Obukhov length L and boundary layer height h, respectively, used in the simulations. To calculate the vertical velocity w_*, the relation $w_*/u_* = (-h/kL)^{1/3}$ was used. It is important to observe that data for experiment 6, with greater resolution, are not available in literature.

Table 1. Friction velocity (m/s) for the different runs and time steps of the Copenhagen experiment. Every time step corresponds at 10 minutes

Run Time step	1	2	3	4	5	7	8	9
1	.36	.68	.46	.56	.58	.48	.65	.72
2	.37	.67	.45	.51	.52	.48	.79	.73
3	.40	.81	.47	.37	.51	.57	.67	.60
4	.43	.68	.39	.44	.58	.62	.67	.59
5	.35	.75	.39	.48	.59	.53	.68	.65
6	.34	.74	.40	.48	.52	.65	.65	.71
7	.42	.76	.40	.39	.52	.63	.68	.73
8	.43	.82	.41	.40	.45	.65	.67	.73
9	.40	.76	.31	.39	.44	.66	.73	.73
10	.37	.73	.34	.39	.44	.62	.73	.66
11	.35	.69	.39	.39	.44	.52	.75	.67
12	.36	.66	.40	.39	.43	.62	.69	.74

Table 2. Monin-Obukhov length (m) for the different runs and time steps of the Copenhagen experiment. Every time step corresponds at 10 minutes

RUN TIME STEP	1	2	3	4	5	7	8	9
1	-26	-178	-152	-75	-492	-71	-71	-793
2	-23	-227	-194	-42	-215	-80	-85	-471
3	-83	-311	-106	-23	-368	-64	-47	-202
4	-42	-160	-101	-32	-735	-111	-49	-366
5	-36	-203	-129	-71	-366	-177	-45	-633
6	-42	-286	-70	-80	-273	-67	-63	-13588
7	-47	-155	-83	-83	-273	-87	-41	-593
8	-38	-228	-60	-101	-262	-71	-47	-471
9	-83	-184	-106	-129	-395	-56	-70	-389
10	-21	-389	-42	-129	-395	-111	-64	-375
11	-32	-133	-101	-129	-395	-215	-52	-262
12	-29	-375	-70	-129	-759	-123	-39	-252

In Figure 1 the observed and predicted scatter diagram is shown. The dash lines indicate that the data are between a factor of two. Both situations, hourly mean values of concentrations and meteorological data, and 20 minutes averaged measured concentrations and 10 minutes averaged values for meteorological data are depicted.

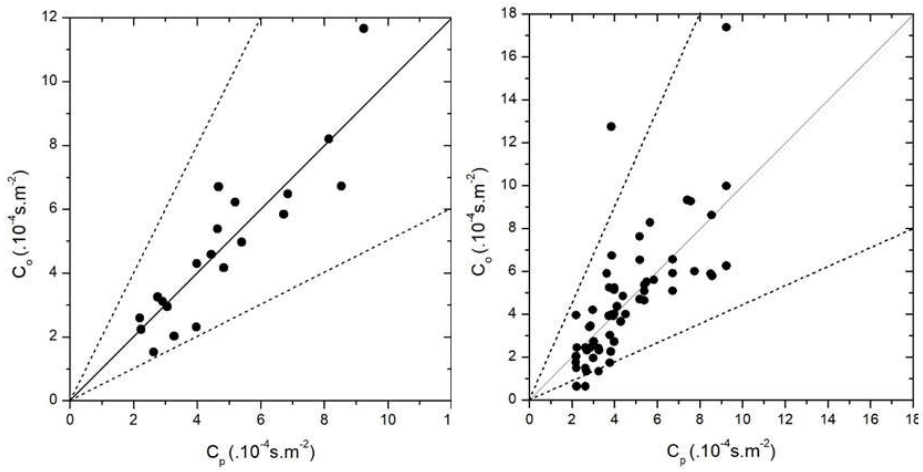

Figure 1. Observed (Co) and predicted (Cp) scatter diagram of crosswind ground-level concentrations using the data of Copenhagen experiment, for the two-dimensional case. At left, data set contains hourly mean values of concentrations and meteorological data. At right, data set with 20 minutes averaged measured concentrations and 10 minutes averaged values for meteorological data. Lines indicate a factor of two

Table 3. Boundary layer height for the different runs of the Copenhagen experiment

RUN	1	2	3	4	5	7	8	9
h (m)	1980	1920	1120	390	820	1850	810	2090

The figure shows that a reasonable agreement is obtained between the experimental data and the new approach. At Table 4 are presented the crosswind ground-level concentrations using the data of Copenhagen experiment, for the two-dimensional case. Data set contains hourly mean values of concentrations and meteorological data. The present model is compared with results presented at Buske *et al*. (2016) by the GILTT method. Statistical comparisons with other methods for the Copenhagen experiment are presented in Table 5. All the models solve the two-dimensional nonstationary advection-diffusion equation and make use of the same parameterizations and experimental data. The GILTT method solves the problem applying the Laplace Transform technique in the time variable (Moreira *et al*., 2006, 2009) and the resulting stationary equation is solved analytically by integral transforms.

Table 4. Observed (Co) and predicted (Cp) crosswind ground-level concentrations using the data of Copenhagen experiment. Data set contains hourly mean values of concentrations and meteorological data. The present model is compared with results presented at Buske *et al*. (2016). The concentrations are normalized by the emission rate

Expt	*Distance (m)*	C_o	$C_{p1\text{ - present}}$	$C_{p2\text{ - GILTT}}$
1	1900	6.48	5.47	7.66
	3700	2.31	3.77	4.35
2	2100	5.38	3.84	5.05
	4200	2.95	2.96	3.41
3	1900	8.2	7.37	8.96
	3700	6.22	5.16	5.62
	5400	4.3	3.98	4.15
4	4000	11.66	9.24	9.47
5	2100	6.72	8.49	9.38
	4200	5.84	6.71	7.37
	6100	4.97	5.39	5.75
7	2000	6.7	3.72	5.09
	4100	3.25	2.63	3.06
	5300	2.23	2.2	2.46
8	1900	4.16	4.26	5.12
	3600	2.02	3.23	3.45
	5300	1.25	2.62	2.72
9	2100	4.58	3.6	4.83
	4200	3.11	2.8	3.26
	6000	2.59	2.18	2.46

Table 5. Statistical comparison between two-dimensional models results, considering hourly mean values of concentrations and meteorological data

model	*nmse*	*cor*	*fa2*	*fb*	*fs*
Present	0.07	0.87	1	0.06	0.19
GILTT	0.06	0.89	1	-0.08	0.09
ADMM	0.15	0.81	0.95	0.18	0.38
M4PUFF	0.21	0.74	0.9	0.1	0.45

Table 6. Crosswind integrated ground-level concentrations, for the three periods of 20 minutes of the second hour pollutant measure of Copenhagen experiment. Co represents the experimental observed concentrations, C_{p1} the predicted concentrations for the present model and C_{p2} the concentrations obtained by the GILTT method (Buske *et al*., 2016). The concentrations are normalized by the emission rate.

	Period I				*Period II*			*Period III*		
Expt	*Distance*	C_o	$C_{p1\text{ - present}}$	$C_{p2\text{ - GILTT}}$	C_o	$C_{p1\text{ - present}}$	$C_{p2\text{ - GILTT}}$	C_o	$C_{p1\text{ - present}}$	$C_{p2\text{ - GILTT}}$
1	1900	5.6	5.84	7.73	8.27	5.66	7.66	5.51	5.5	7.59
	3700	1.74	3.77	4.29	2.25	3.82	4.37	3.02	3.78	4.38
2	2100	4.36	4.1	5.12	3.97	3.97	5.04	6.73	3.87	5
	4200	2.72	3.02	3.44	1.96	3	3.41	4.2	2.97	3.37
3	1900	6	7.74	9.05	9.26	7.57	8.96	9.32	7.41	8.87
	3700	4.7	5.19	5.59	6.53	5.18	5.64	7.62	5.17	5.64
	5400	3.93	3.93	4.07	5.24	3.98	4.17	4.01	3.98	4.21
4	4000	6.26	9.24	9.44	9.97	9.24	9.48	17.37	9.24	9.48
5	2100	5.78	8.57	9.48	8.62	8.54	9.38	5.89	8.5	9.27
	4200	5.09	6.72	7.35	6.55	6.72	7.39	5.91	6.72	7.37
	6100	5.07	5.39	5.64	5.37	5.39	5.78	4.65	5.39	5.82
7	2000	2.72	3.98	5.16	12.74	3.85	5.09	5.25	3.74	5.03
	4100	2.31	2.71	3.08	1.34	2.68	3.06	2.42	2.64	3.03
	5300	2.45	2.23	2.46	0.64	2.22	2.46	1.49	2.2	2.45
8	1900	4	4.51	5.16	4.84	4.39	5.12	3.65	4.29	5.07
	3600	2.31	3.27	3.47	1.34	3.25	3.45	2.42	3.24	3.43
	5300	2.45	2.63	2.72	0.64	2.63	2.72	1.49	2.62	2.71
9	2100	3.98	3.86	4.9	3.93	3.73	4.83	5.9	3.63	4.77
	4200	3.46	2.88	3.29	2.44	2.84	3.26	3.4	2.81	3.22
	6000	3.96	2.19	2.46	2.04	2.19	2.46	1.76	2.18	2.44

Table 7. Statistical comparison between two-dimensional models results, considering periods of 20 minutes average pollutant concentration

Model	NMSE	COR	fa2	fb	fs
Present	0.2	0.73	0.92	0.03	0.38
GILTT	0.17	0.75	0.9	-0.1	0.28

The final concentration is obtained by numerical inversion in time. The ADMM model of Moreira *et al*. (2005) is obtained by a Laplace Transform technique with numerical inversion considering the PBL as a multilayer system where in each layer the eddy diffusivity and wind are constants. The M4PUFF model (Tirabassi and Rizza, 1997) is based on a general technique for solving the K-equation, using the truncated Gram-Charlier expansion of the concentration field and finite set equations for the corresponding moments. The statistical indices (Hanna, 1989; Chang and Hanna, 2004) in Table 5 point out that these models simulate satisfactorily the observed concentrations, regarding the *nmse* (normalised mean square error), *fb* (fractional bias) and *fs* (fractional standard deviation) values relatively near to zero and *cor* (correlation coefficient) and *fa2* (factor of two) relatively near to 1. Table 5 also permits to stress that the new model and the GILTT results present similar values for *nmse*, *cor* and *fa2*.The great advantage here is the avoid of the numerical inversion in time from the previous works, which allows us to obtain the final result much faster. Running both models together, in a simple i5 notebook of 64 bits, for n=100 eigenvalues, the complete results of tables 4 and 5 were obtained with the new model until only the result for one distance was obtained for the GILTT method with numerical inversion. Table 6 present the crosswind integrated ground-level concentrations, for the three periods of 20 minutes of the second hour pollutant measure of Copenhagen experiment. The present model is compared with results presented at Buske *et al*. (2016) by the GILTT method. The concentrations are normalized by the emission rate. Table 7 again permits to stress that the new model and the GILTT results present similar values for *nmse*, *cor* and *fa2*, showing the similarity between the models, except for numerical inversion and computational time.

Conclusions

We begin our final analysis of the proposed method, underlining that the reported solution is analytical, in the sense no appoximation is made along the solution derivation except for the round-off error. The concentration can be evaluated at any time due the analytical shape of the solution and as a consequence, this methodology demands less computational effort. The consistency here is shown by comparison with crosswind integrated experimental data and the very good results attained, under statistical point of view, must be emphasized. Moreover, the analytical character and simplicity of the solution, reinforces that the proposed method is a robust and promising method to simulate pollutant dispersion in atmosphere. The focus of the future works will be on extend this investigation to simulate centerline concentrations, as well as investigate other scenarios of interest to the area.

Acknowledgements

The authors thank to the Coordenação de Aperfeiçoamento de Pessoal de Ensino Superior (CAPES), Conselho Nacional de Desenvolvimento Científico e Tecnológico (CNPq) and the Fundação de Amparo à Pesquisa do Estado do Rio Grande do Sul (FAPERGS) by the partial financial support to the development of this research.

REFERENCES

Buske, D., Vilhena, M.T., Bodmann, B. and Tirabassi, T., 2012a. Analytical Model for Air Pollution in the Atmospheric Boundary Layer. Air Pollution - Book 1, InTechOpen, pp. 39-58.

Buske, D., Vilhena, M.T., Tirabassi, T. and Bodmann, B., 2012b. Air pollution steady-state advection-diffusion equation: the general three-dimensional solution. Journal of Environmental Protection, Vol. 3, pp. 1124–1134.

Buske, D., Vilhena, M.T. and Moreira, D.M., 2016. Solução GILTT Bidimensional em Geometria Cartesiana: Simulação da Dispersão de Poluentes na Atmosfera (In Portuguese). Saarbrucken: Novas Edições Acadêmicas.

Chang, J. and Hanna, S., 2004. Air quality model performance evaluation. *Meteorology and Atmospheric Physics*, Vol. 87, pp. 167-196.

Cotta, R. and Mikhaylov, M., 1997. Heat conduction lumped analysis, integral transforms, symbolic computation, John Wiley Sons, Baffins Lane, Chinchester, England.

Degrazia, G.A., Campos Velho, H.F. and Carvalho, J.C., 1997. Nonlocal exchange coefficients for the convective boundary layer derived from spectral properties. Contributions to Atmospheric Physics, Vol 70, No. 1, pp. 57-64.

Gryning, S.E. and Lyck, E., 1984. Atmospheric dispersion from elevated source in an urban area: comparison between tracer experiments and model calculations. *Journal of climate Applied Meteorology*, Vol. 23, pp. 651-654.

Gryning, S.E., Holtslag, A.M.M., Irwin, J. and Sivertsen, B., 1987. Applied dispersion modelling based on meteorological scaling parametres. *Atmospheric Environment*, Vol. 21, pp. 79-89.

Hanna, S.R., 1989. Confidence limit for air quality models as estimated by bootstrap and jacknife resampling methods. *Atmospheric Environment*, Vol. 23, pp. 1385-1395.

Irwin, J.S., 1979. A theoretical variation of the wind profile power-law exponent as a function of surface roughness and stability. *Atmospheric Environment*, Vol. 13, pp. 191-194.

Moreira, D.M., Rizza, U., Vilhena, M.T. and Goulart, A., 2005. Semi-analytical model for pollution dispersion in the planetary boundary layer. *Atmospheric Environment*, Vol. 39, No. 14, pp. 2689-2697.

Moreira, D.M., Vilhena, M.T., Buske, D. and Tirabassi, T., 2006. The GILTT solution of the advection-diffusion equation for an inhomogeneous and nonstationary PBL. *Atmospheric Environment*, Vol. 40, pp. 3186–3194.

Moreira, D.M., Vilhena, M. T., Buske, D. and Tirabassi, 2009. The state-of-art of the GILTT method to simulate pollutant dispersion in the atmosphere. *Atmospheric Research*, Vol. 92, pp. 1–17.

Panofsky, H.A. and Dutton, J.A., 1988. Atmospheric Turbulence. John Wiley & Sons, New York.

Seinfeld, J.H. and Pandis, S.N., 1998. Atmospheric chemistry and physics of air pollution. John Wiley & Sons, New York.

Tirabassi, T. and Rizza, U. 1997. Boundary layer parameterization for a non-Gaussian puff model. *Journal of Applied Meteorology,* Vol. 36, pp. 1031-1037.

Vilhena, M.T., Buske, D., Degrazia, G.A. and Quadros, R.S., 2012. An analytical model with temporal variable eddy diffusivity applied to contaminant dispersion in the atmospheric boundary layer. Physica A, Vol. 391, pp. 2576-2584.

Wortmann, S., Vilhena, M.T., Moreira, D.M. and Buske, D., 2005. A new analytical approach to simulate the pollutant dispersion in the PBL. *Atmospheric Environment,* Vol 39, No. 12, pp. 2187-2194.

****